

Diel patterns in nitrate NO_3^- concentration suggest importance of microbial pathways for produced by in-stream processing processes

Jan Greiwe¹, Markus Weiler¹, Jens Lange¹

¹Hydrology, University of Freiburg, Fahnbergplatz Friedrichstraße 39, 79098 Freiburg, Germany

5

Correspondence to: Jan Greiwe (jan.greiwe@hydrology.uni-freiburg.de)

Abstract. Diel cycles in stream nitrate NO_3^- concentration represent the sum of all processes affecting nitrate NO_3^- concentration along the flow path. Being able to partition diel nitrate NO_3^- signals into portions related to different biochemical processes would allow to calculate calculation of daily rates of such processes that are urgently needed for water quality predictions. In this study, we analyzed aimed to identify distinct diel nitrate patterns in high-frequency NO_3^- monitoring data and investigated the origin of these patterns. Monitoring was performed at three locations in a 5.1-km long stream reach draining a 430 km², mainly forested but anthropogenically influenced² catchment during one growing season. We tested if the observed diel variability in nitrate concentration and resulted from upstream sources and subsequent downstream transport or emerged simultaneously along the stream. We determined in 355 complete daily recordings on which we performed a k-means cluster analysis. We compared travel time estimates to time lags between observations at the monitoring sites by cross-correlation to differentiate between in-stream and transport control on diel NO_3^- patterns. We found that time travel time failed to explain the observed lags were closer to zero than travel time estimation assuming plug flow suggested and concluded that ubiquitous in-stream processes prevailed in the creation of diel variability. To further analyze the diel nitrate signals we used k-means clustering to identify patterns in the diel portion of nitrate concentrations and interpreted the resulting clusters with regard to potential drivers and the calculated nitrate balance of sub-reaches. We found that At least 70% of all diel patterns were attributed to clusters negatively related to the diel course of insolation with highest nitrate amplitudes on warm and sunny days and low water levels. We argue that temporal shifts towards the remaining clusters are rather due to shifts in microbial nitrate processing than reflected shapes typically associated with photoautotrophic NO_3^- assimilation. The remaining patterns suggested that other biochemical (e.g. nitrification and denitrification) or physical processes (lateral inputs) contributed to the formation of diel NO_3^- patterns. Seasonal trends in photosynthesis driven plant uptake. These results diel patterns suggest that the magnitude of microbial nitrate processing may be large compared to plant uptake relative importances of the contributing processes varied throughout the year.

10

15

20

25

1 Introduction

30 In-stream processing of nutrients can significantly influence loads and concentrations transported to receiving ecosystems (Roberts and Mulholland, 2007). Nutrients are temporally taken up and immobilized (Peterson et al., 2001; Roberts and Mulholland, 2007). Nutrients are repeatedly taken up and released again by organisms during downstream transport, a concept known as “nutrient spiraling” (Ensign and Doyle, 2006) (Ensign and Doyle, 2006). Thus, depending on the rates of nutrient uptake and release, in-stream nutrient processing may reduce the risk of harmful eutrophication (Birgand et al., 2007). As a result of human activity, many streams nowadays exhibit increased levels of nitrogen (Dodds and Smith, 2016). Among the different N-species, NO_3^- (nitrate) (NO_3^-) is of special interest since it usually represents the largest fraction in dissolved inorganic nitrate (DIN) and it is nowadays easily detectable using in-situ spectrometer probes. At the same time, water quality management requires knowledge of nitrate processing rates to predict how rapidly nitrate inputs will be transformed and attenuated. This is particularly important in light of changing climatic conditions and possible associated drought periods (Austin and Strauss, 2011). Nitrogen (DIN) and is nowadays easily detectable using in-situ optical spectrometer probes. At the same time, water quality management requires knowledge of NO_3^- processing rates to predict how rapidly NO_3^- inputs are transformed and attenuated. This is particularly relevant in light of a changing climate and a predicted reduction of summer flow (Austin and Strauss, 2011; Mosley, 2015; Hellwig et al., 2017).

45 Similar to other solutes, e.g. dissolved oxygen (DO) or CO_2 , nitrate concentrations exhibit diel (i.e. with a period of 24 h) cycles. The increasing body of high frequency nitrate monitoring data resulting from availability of optical in-situ probes shows that such diel cycles are not ubiquitous. Some streams consistently exhibit strong diel patterns (Heffernan and Cohen, 2010), others do so only during certain seasons (Rusjan and Mikoš, 2010; Aubert and Breuer, 2016; Schwab, 2017), still others do not present diel patterns at all (Duan et al., 2014). Complementary to other approaches such as stable isotope studies (Pellerin et al., 2009; Mulholland et al., 2009; Cohen et al., 2012; Gammons et al., 2010), nutrient addition experiments (Covino et al., 2010), and benthic chambers (Hensley and Cohen, 2020), analysis of diel nitrate cycles can be used to quantify processing rates (Heffernan and Cohen, 2010; Rode et al., 2016). Diel nitrate cycles can be described as the convolution of upstream boundary conditions and processes occurring along spatially heterogeneous flow paths (Hensley and Cohen, 2016). Correspondingly, this method aims at estimating rates of individual processes by deconvolving the nitrate concentration time series. This requires prior knowledge on the timing of the involved processes, including biochemistry, transport and external inputs.

Biochemical processes influencing nitrate concentration include nitrate depletion via denitrification and uptake by both autotrophs (U_A) and heterotrophs, as well as production via mineralization and subsequent nitrification. These processes depend on environmental conditions and are interrelated with stream metabolism on a fine temporal scale (Burns et al., 2019). Due to photosynthetic light requirements, U_A can be considered zero at night (Heffernan and Cohen, 2010) and conceptualized

as a function of insolation (Hensley and Cohen, 2016). This restriction has been used to partition the difference between observed nitrate concentrations and an interpolated baseline into U_A and microbial net depletion (Heffernan and Cohen, 2010), assuming all other processes to be constant. However, there is evidence that diel variation may not only be influenced by U_A .
65 In many systems, diel variability has also been found in rates of nitrification and denitrification (Laursen and Seitzinger, 2004; Dunn et al., 2012; Scholefield et al., 2005), e.g. due to changing oxygen levels in sediments (Christensen et al., 1990). Such diel variability in microbial nitrate processing would cause the above partitioning approach to fail (Kunz et al., 2017).

~~In flowing waters, biochemical processes are superposed with downstream transport. The solute signal measured at any
70 location integrates over all conditions and events that water parcels passing that location were previously exposed to. Correspondingly, the benthic footprint, i.e. the upstream area influencing concentrations at the measurement point, depends on the flow velocity and the solute turnover rate. While gaseous solutes like DO may quickly equilibrate with the atmosphere, upstream discontinuities in nitrate (e.g. tributary confluxes, lakes or reservoirs, groundwater or waste water inputs) may persist further downstream (Hensley and Cohen, 2016). In open systems with unknown upstream boundary condition, it is therefore
75 a priori unclear whether observed diel patterns are produced by conditions in the associated stream reach or at some upstream origin from which they are advected downstream.~~

~~In the present study~~ Similar to other solutes, e.g. dissolved oxygen (DO) or carbon dioxide (CO_2), NO_3^- concentrations can exhibit diel (i.e. 24 h) cycles. However, the increasing body of high frequency NO_3^- monitoring data from optical in-situ probes
80 shows that such diel cycles are not ubiquitous. Some streams consistently exhibit strong diel patterns (Heffernan and Cohen, 2010), while others do so only during certain seasons (Rusjan and Mikoš, 2010; Aubert and Breuer, 2016; Schwab, 2017; Rode et al., 2016), and still others do not show diel patterns at all (Duan et al., 2014). Biochemical processes influencing NO_3^- concentration include NO_3^- depletion via denitrification and photoautotrophic uptake, as well as production via mineralization and subsequent nitrification. Previous studies have suggested that diel variation in stream NO_3^- concentration are mainly related
85 to in-stream photoautotrophic uptake (Nimick et al., 2011; Burns et al., 2019). Due to photosynthetic light requirements, photoautotrophs take up NO_3^- mostly during the day (Mulholland et al., 2006), which causes minimum and maximum NO_3^- concentrations to typically occur in the late afternoon and in the early morning (prior to sunrise), respectively. However, there is evidence that diel variation may not be influenced by photoautotrophic uptake alone. In many systems, diel variability has also been found in rates of nitrification and denitrification (Laursen and Seitzinger, 2004; Dunn et al., 2012; Scholefield et al.,
90 2005), e.g. due to changing oxygen levels in sediments (Christensen et al., 1990).

In flowing waters, biochemical processes are superposed by downstream transport. Therefore, the solute signal measured at a specific location integrates over all conditions and events that water parcels were previously exposed to. As a result, the benthic footprint, i.e. the upstream area influencing concentrations at the measurement point, depends on flow velocity and solute turnover rate. While gaseous solutes like DO may quickly equilibrate with the atmosphere, upstream discontinuities in NO_3^-
95 (e.g. tributary confluxes, lakes or reservoirs, groundwater or waste water inputs) may persist further downstream (Hensley and

Cohen, 2016). In open systems with unknown input signals, it is therefore unclear whether diel concentration patterns are produced by conditions in the investigated stream reach (in-stream control) or stem from upstream sources (Pellerin et al., 2009) and are transported downstream (transport control).

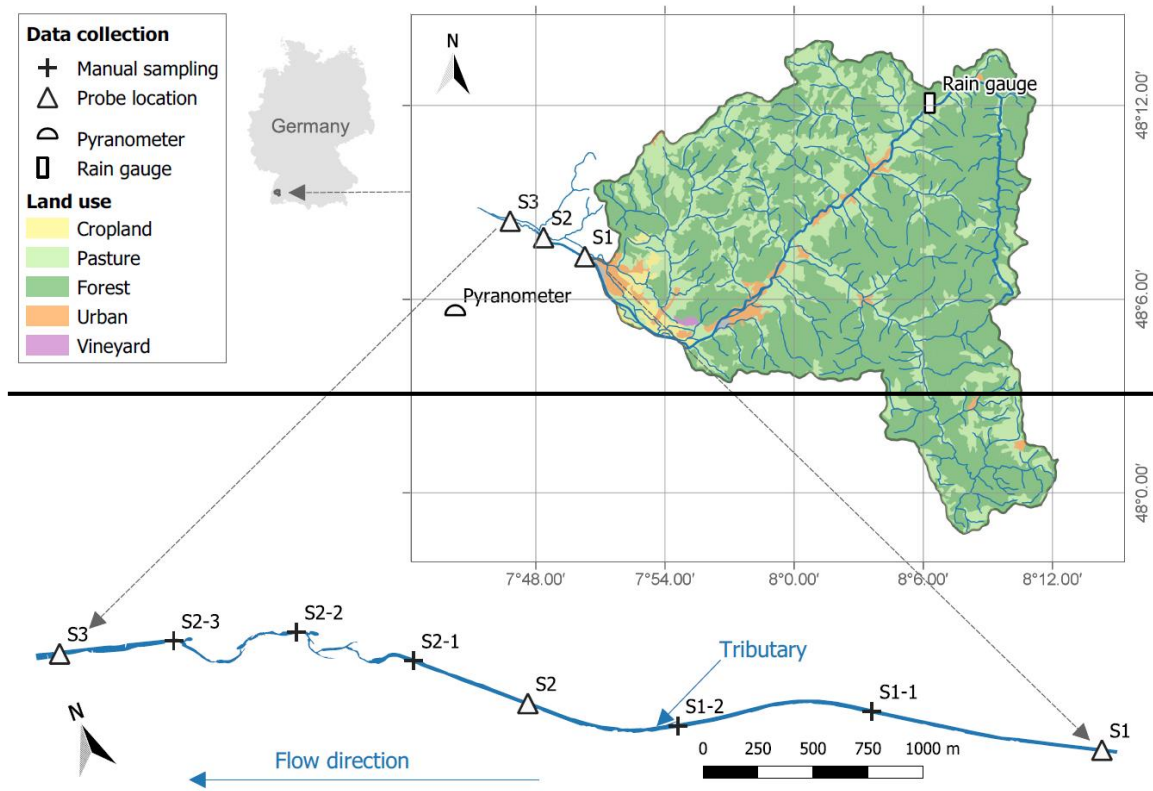
Here we analyze ~~diel nitrate patterns~~ high-frequency NO_3^- data observed at three ~~connected~~ monitoring sites along ~~delimiting~~ two reaches in the lower course of the river Elz in Southwest Germany. We hypothesize that (1) ~~diel nitrate cycles in the investigated system are predominantly produced by in-stream conditions and (2) are indicative of daily net nitrate processing in the stream sub-reaches. We test our first hypothesis~~ We aim to investigate, (1) if there are diel patterns in NO_3^- concentration, (2) if these patterns are subject to in-stream or transport control, and (3) how they are related to environmental conditions and potential drivers. In order to address these questions, we performed a cluster analysis on high-frequency NO_3^- recordings. We further differentiated between in-stream and transport control by comparing travel time estimates to time lags between concentration signals at adjacent monitoring sites to benchmark travel time determined by a conservative tracer injection. In order to test the second hypothesis, we analyze the different diel patterns present in the monitoring data, under which conditions they emerge, and how they are related to nitrate balances of the sub-reaches. Finally, we compared environmental conditions among clusters and determined correlations between the concentration rates of change and potential drivers of biochemical processes.

2 Methods

2.1 Study site

The studied stream reach is located in the lower course of the river Elz in Southwest Germany between the municipalities of Emmendingen and Riegel (Figure 1). At our study site the river Elz drains an area of approximately 430 km² of which 66% are forested forest and 21% are grassland. The fraction of cropland is below 2%. The catchment river contains ~~man-made structures including~~ several weirs and ~~one~~ receives inflows from a small wastewater treatment plant about approximately 25 km upstream of the study site. ~~Most~~ Yet, most wastewater, ~~however,~~ of the upstream catchment is collected in transferred to a larger large treatment plant located further downstream. The monitored stream reach section spans a distance of 5.1 km and is subdivided divided into two sub-reaches with different morphology. ~~While the upstream~~ The upper reach (2.7 km) is characterized by a uniform gravel bed which is straightened and protected against erosion by regularly spaced groundills and in this sense is representative of many rivers in Southwest Germany, the downstream sub-. The lower reach (2.4 km) was subject to extensive revitalization measures including flood dam relocation and installation of a near-natural meandering river course. ~~The constructions~~ Revitalization measures were completed in 2016 and since then natural dynamics are controlling its have controlled river morphology. Both sub-reaches are characterized by a largely open canopy canopies and shallow water depth (usually below 0.4 m, allowing) water depths, which allows light to reach the stream bed. However, in the downstream sub-reach water depth is depths are more variable, so that depths exceed exceeding 1.5 m at some locations. This pattern

corresponds to an increased variability in As a consequence, also flow velocities are more variable in the downstream sub-reach. Both reaches are scarcely colonized by macrophytes and filamentous algae and a visible biofilm develops on the gravel bed, particularly in the second half of the growing season. There are no obvious influxes along the two stream reaches, except for a minor tributary enters in the upstream sub-reach, its influence on the results of this study is discussed later. (Fig. 1).



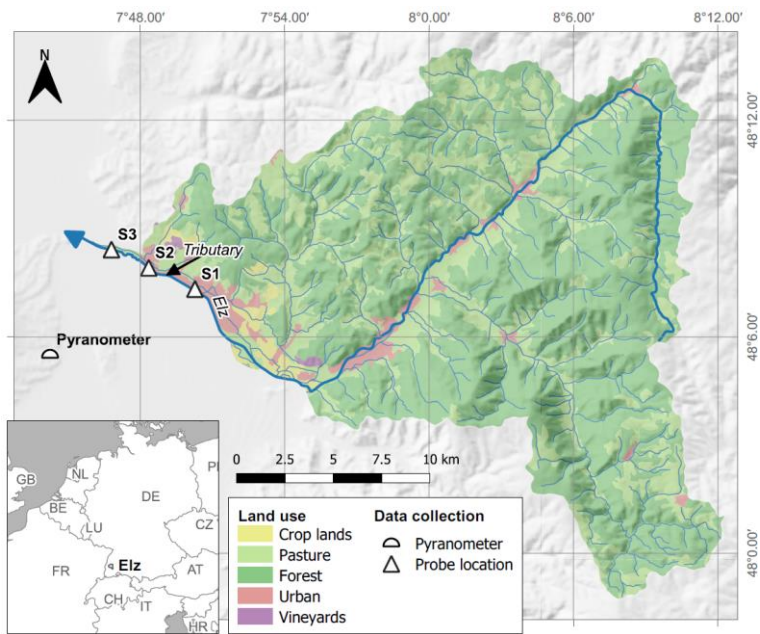


Figure 1: Location of monitoring points along the stream reach and land use in the contributing catchment.

135 2.2 Data collection

~~Nitrate concentration~~ Concentration of NO_3^- was measured at 15 ~~minute~~ min intervals at the three monitoring sites using UV-Vis spectrometer probes (spectro::lyser, s::can Messtechnik GmbH, Vienna, Austria) from April to November in 2019. As only two spectrometer probes were available, one probe was periodically repositioned so that input and output concentrations of either the upper or the lower stream reach were measured. In addition to the in-situ measurements, biweekly grab samples were collected at eight locations along the studied stream reach, including the probe locations, to provide a local calibration for probe measurements (Fig. S1) and to assess longitudinal concentration profiles and validate probe measurements evolution between monitoring sites. Samples were analyzed using ion chromatography (Dionex ICS-1100, Thermo Fisher Scientific Inc., USA). Stream temperature (T) and water levels (h) were continuously recorded at site S3 (TD-Diver, Van Essen Instruments, Netherlands) at 15 minute intervals. Discharge was calculated using a rating-curve based on two local NaCl tracer injections during stationary flow conditions, data of which was provided measurements by the local regional water agency authority, and one additional tracer test salt dilution measurement during elevated higher water levels on 15 November 15th-2019 (> 70 % of recorded water levels). In the latter tracer test dilution measurement we injected 33 kg of NaCl at site S1 so that to cover both sub-reaches were covered. Solar radiation data was obtained. We used global irradiance (S) data from a nearby climate station at the nearby (<< 10 km) Lochernbach experimental site in Eichstetten, Fig. 1) as a measure of sunlight intensity.

2.3.1 Assessing the origin of diel nitrate variation

If diel nitrate variation originated from some upstream source and subsequent downstream transport, time lags should be detectable between nitrate signals at adjacent monitoring points that correspond to solute travel times between these points. In order to exclude an external source for diel nitrate patterns we determined the time lags between nitrate signals by means of cross correlation which is a standard method for determining temporal shifts between signals (Derrick and Thomas, 2004) and compared them to the tracer travel time (τ_a) and the nominal water residence time (τ) according to Kadlec (1994). While τ_a is the first moment of the tracer residence time distribution, τ is the ratio of reach volume and discharge. We determined reach volume from water level recordings at S3 and observations of channel width. In order to account for variability in channel geometry, we estimated minimum and maximum values of τ using rough estimates of channel widths between 20 and 25 m in the lower sub reach and 15 to 20 m in the upper sub reach. Time lags obtained from cross correlation were tested for difference from zero using two sided t tests.

2.3.2.3.1 Identification and characterization of diel patterns in NO_3^- concentration

We used k-means cluster analysis to identify and classify diel patterns in stream NO_3^- concentrations as done previously by Aubert and Breuer (2016). This method partitions a data set into a pre-defined number of k clusters by iteratively minimizing the within cluster sum of squares. We used the algorithm by Hartigan and Wong (1979) that is implemented in the 'stats' R-package. We used k means cluster analysis to identify and classify diel patterns in stream nitrate concentrations as done previously by Aubert and Breuer (2016). This method partitions a data set into a pre defined number of k clusters by iteratively minimizing the within cluster sum of squares. We used the algorithms by Hartigan and Wong (1979) that is implemented in the 'stats' R package (R Core Team, 2019). In order to ensure that the resulting clusters represented variability in diel cycles and not in nitrate background concentrations the analysis was done on the diel portion of the solute concentration signal, hereafter referred to as residual concentration (C_{res}). Residual concentrations were obtained by subtracting a 24 hour centered moving average from the measured concentrations (C_{obs}) and smoothed by applying a moving average of 2 hours. One feature of the k means method that introduces some degree of subjectivity is the determination of number of clusters k. We therefore tested cluster numbers ranging between 2 and 20 and determined the best partition by both assessment of explanatory benefit per additional cluster, also known as 'elbow method', and visual inspection of clusters. The elbow method was not clearly indicative, however, we opted for six clusters as higher values of k did not produce new clusters in terms of timing but rather caused further splitting of existing clusters by amplitude. The input to this algorithm is a matrix whose rows represent elements to be partitioned (days in the present case) and whose columns represent the dimensions according to which the elements are compared. In the present case, these dimensions correspond to the time of day of the measurements ($n=96$ at a measurement interval of 15 minutes). More information about the method can be found in e.g. Tan et al. (2019).

In order to further characterize the identified diel patterns, we assessed environmental conditions during the occurrence of the respective clusters. Particularly, we compared daily average and amplitude of nitrate concentration, average of water levels (h_{mean}), solar radiation (S_{mean}) and water temperature (T_{mean}). We further investigated the relationship of diel patterns to diel signals of potential drivers, i.e. insolation and water temperature. Diel nitrate cycles reflect the time varying balance between nitrate inputs and producing and depleting processes, e.g. nitrate concentration increases the quickest when nitrate production is most dominant. This means that potential drivers should be correlated to the rate of change of C_{res} , i.e. to its first derivative δC_{res} . Correspondingly, we related δC_{res} to the observed diel signals of insolation (S) and water temperature (T) by calculating daily Spearman rank correlation coefficients. Another potential driver of diel solute cycles is discharge variation. In contrast to the above drivers of biochemical processes, discharge would directly affect solute concentration. For example, if stream water was diluted by rainfall, maximum discharge and minimum concentration would occur simultaneously and not be mediated by the rate of a process. We therefore expected a potential relationship of discharge with C_{obs} rather than with δC_{res} . Correspondingly, we assessed the potential effect of diel variation in discharge by correlating C_{obs} to water level recordings (h), avoiding uncertainties from rating curve extrapolation.

2.3.3 Assessing the relation of diel patterns to the nitrate balance

The influence of diel patterns on the stream nitrate budget was assessed by calculating both temporal and spatial net change. As sub reach balance we understand the difference between daily means of nitrate concentration at an upstream (C_{up}) and downstream (C_{down}) monitoring site, thus exclusively representing changes that happen in the stream reaches between these points:

$$\Delta C = C_{\text{down}} - C_{\text{up}}. \quad (1)$$

The analysis was done on the diel portion of the solute concentration signal, hereafter referred to as diel concentration (C_{diel}), to ensure that the resulting clusters represented variability in diel cycles and not in NO_3^- background concentrations. Residual concentrations were obtained by subtracting a 24 hour centered moving average from the measured concentrations (C_{obs}) and smoothed by applying a moving average of 2 hours. One feature of the k-means method that introduces some degree of subjectivity is the determination of the number of clusters k. We therefore tested k values between 2 and 20 and determined the best partition by both an assessment of explanatory benefit per additional cluster, also known as ‘elbow method’, and by visual inspection of clusters. The elbow method was not clearly indicative as no sharp bent was observed. Instead, we visually found an optimum number of six clusters, since higher values of k did not produce new clusters in terms of timing but rather caused further splitting of existing clusters by amplitude.

Besides the diel scale, patterns in NO_3^- concentration may also vary seasonally and longitudinally. We therefore assessed the relationship of absolute NO_3^- concentrations and intensity of diel patterns to environmental conditions by determining Spearman rank correlations of daily means of C_{obs} and daily NO_3^- amplitudes with global irradiance (S), water temperature (T), and, water level (h). As a measure for longitudinal stability of diel patterns, we calculating the fraction of days on which diel patterns at the upstream and downstream monitoring sites were assigned to the same cluster.

2.3.2 In-stream vs. transport control on diel NO_3^- patterns

In order to differentiate between in-stream and transport control on diel NO_3^- patterns, we determined time lags between adjacent monitoring sites by cross-correlation analysis and compared these to estimated solute travel time. If diel NO_3^- variation originated from some upstream source and subsequent downstream transport, time lags between sites should correspond to solute travel times. In contrast, if diel patterns were produced by in-stream processes simultaneously at all points along the flow path, we expected the time lag to be zero in most instances. Cross-correlation analysis is a standard method to determine time lags between signals (Derrick and Thomas, 2004). It is based on the idea that the strength of a correlation between two signals changes according to a temporal shift. The shift that maximizes the strength of the correlation is considered the time lag between the signals. This method works best, if the two signals have a similar shape, i.e. they are strongly correlated at an optimal lag. We therefore determined time lags only for days when the correlation coefficient r between up and downstream sites exceeded 0.75. This was true for 121 out of 144 days with complete measurements at both the upstream and the downstream monitoring site.

Time lags were compared to two independent estimates of solute travel time: mean tracer travel time (τ_a) and nominal water residence time (τ_n) according to Kadlec (1994). While τ_a is the first moment of the tracer residence time distribution and was determined from the breakthrough curves of the salt dilution measurements, τ_n is the ratio of reach volume and discharge. In contrast to τ_a , which requires tracer data as an input and could only be determined for our own dilution measurement (raw data of low flow measurements was not available from the regional water authority), τ_n was calculated continuously from water level recordings and channel width. As discharge, water depth, and channel width vary along the stream reach, we decided to account for variability in channel geometry and flow conditions by estimating a range of likely travel times based on channel width. Channel widths were estimated from aerial imagery and ranged from 20 to 25 m in the lower sub-reach and from 15 to 20 m in the upper sub-reach. Time lags obtained from cross-correlation were tested for difference from zero using t-tests and for difference from travel time estimates using paired t-tests.

2.3.3 Characterization of clusters

In order to characterize the clusters, we compared environmental parameters during the occurrence of the respective clusters. We particularly assessed daily means of NO_3^- concentration, water levels (h_{mean}), and water temperature (T_{mean}) as well as the daily maximum solar irradiance (S_{max}). The relationships between clusters and potential drivers were investigated by

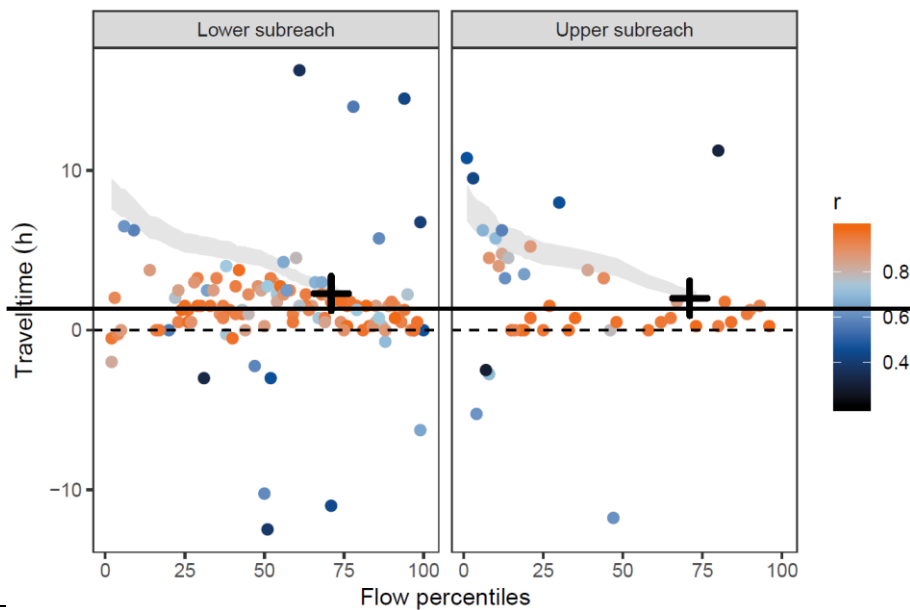
calculating daily Spearman rank correlations between C_{diel} and the diel course of the drivers. As potential drivers we considered global irradiance (S), water temperature (T) and discharge, the latter represented by water level (h). These environmental parameters are usually considered to influence the rate of biogeochemical processes, i.e. the rate of change of NO_3^- concentration rather than instantaneous NO_3^- concentration. Laboratory experiments have shown such behavior for the effect of light on NO_3^- uptake rates of algae (Grant, 1967) or the effect of temperature on denitrification rate (Pfenning and McMahon, 1997). We therefore assessed correlations between drivers and the first derivative (δC_{diel}) of the diel concentration signal C_{diel} . This corresponds to the way biochemical processes are implemented in some recent solute models (Hensley and Cohen, 2016; Grace et al., 2015). However, changes in water level may affect NO_3^- concentrations both indirectly, e.g. by influencing hyporheic exchange and biochemical processes therein (Trauth and Fleckenstein, 2017), and directly, since additional flow components may be enriched or depleted in NO_3^- compared to pre-event water. In the case of water level, we therefore calculated correlations with both C_{diel} and δC_{diel} .

3 Results

~~3.1 Prevalence of in-stream processes in creation of diel patterns~~

3.1 Variability of diel patterns in space and time

The benchmark tracer injection at a water level of 15.4 cm and a corresponding discharge of $2.0 \text{ m}^3 \text{ s}^{-2}$ resulted in travel time estimates of 2.0 h in the upper and 2.3 h in the lower sub-reach, while time lags of nitrate determined by cross correlation were very variable. We considered lags between signals with strong cross correlation more reliable than for signals with a weak or no correlation. Lags resulting from strong cross correlation ($r > 0.75$) ranged between zero and travel time estimates from both the tracer injection and nominal water residence time (Figure 2), indicating that time lags were shorter than solute travel time. Thus, time lags were usually too small to be considered the result of advective downstream transport of the concentrations signal. At the same time, lags were statistically different from zero (both sub-reaches $p < 0.001$ in two-sided t tests).



265 **Figure 2: Travel time between diel nitrate signals at adjacent monitoring points compared to the tracer travel time (black crosses) and the range of estimated nominal travel time (shaded area). Color of the dots indicates strength of cross-correlation.**

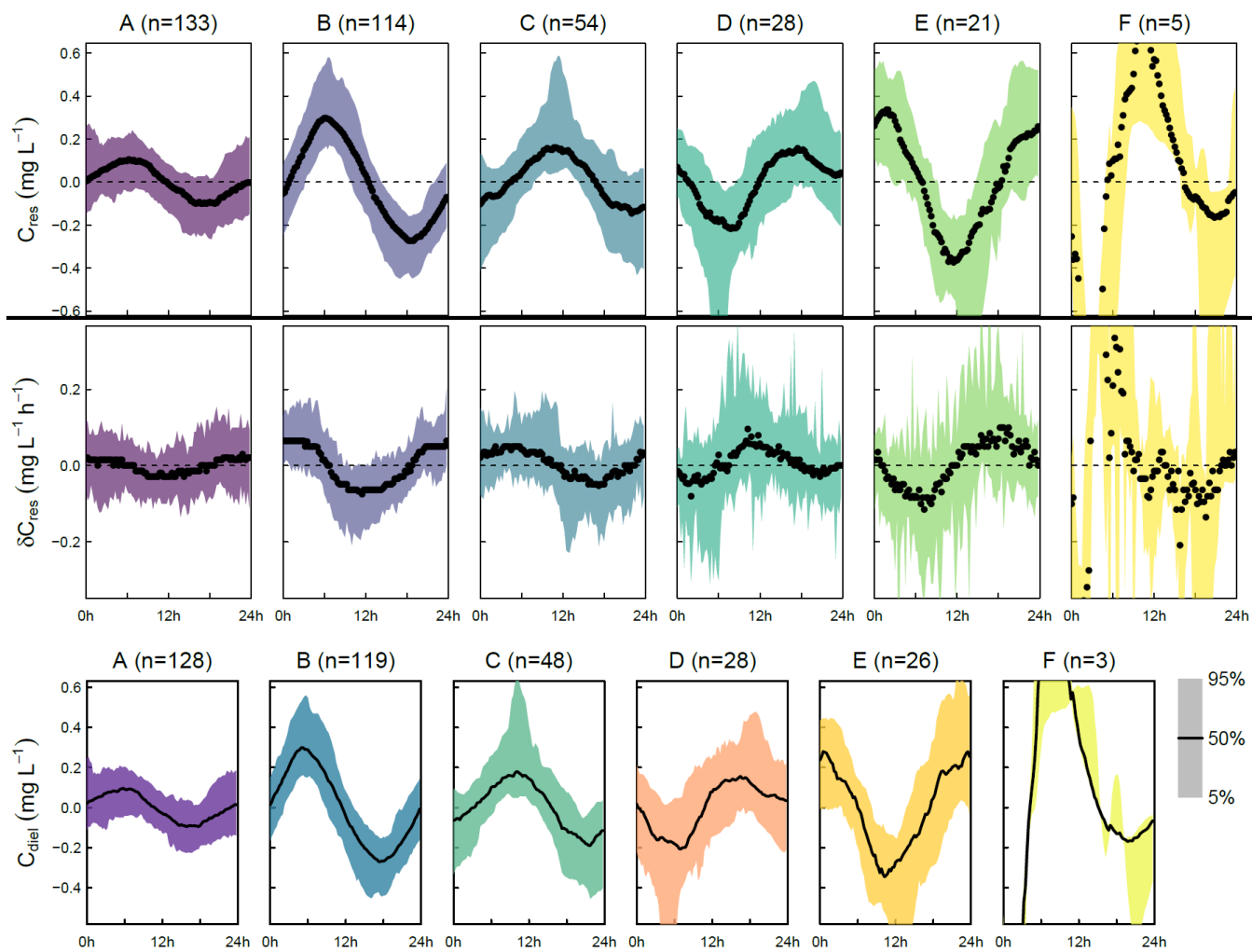
3.2 Diversity in diel patterns

Data collection at the three monitoring sites resulted in 355352 complete diel nitrate NO_3^- signals, almost all of which showed a diel pattern (Figure 3). The cluster analysis resulted in 6 clusters that clearly differed in terms of amplitude and timing of minimum and maximum concentrations. 70 (Fig. 2). 69.6% of the days were attributed to the clusters A ($n=132128$) and B ($n=115119$) which both reached peak concentration in the early morning and minimum concentration in the late afternoon, but the daily amplitude was higher in cluster B. The remaining clusters were characterized by peaks around midday (cluster C, $n=5448$), in the afternoon (cluster D, $n=28$) and around midnight (cluster E, $n=2126$). The last cluster (cluster F, $n=3$) did not include enough days ($n=5$) for a proper characterization. The medians of clusters A to E roughly represented sine waves shifted in phase by a quarter of a period (0.5π) or 6 hours in units of Average time. Correspondingly, of the derivatives of the clusters preceded the residuals by another quarter of a period. Note that δC_{res} was the rate of daily concentration change of the diel portion of the concentration signal (C_{res}). maxima in clusters A to E were 4:33 h, 5:32 h, 10:18 h, 16:44 h, and not of observed concentrations (C_{obs}). The change rate of diel residuals resembled the signal shape of potential drivers of diel patterns but may differ in absolute terms as it was determined from the detrended data. Particularly the fact that its sign switches between positive 23:33 h, respectively. The respective average times of daily minima were 17:46 h, 17:36 h, 21:39 h, 6:06 h, and negative does not imply that the direction of associated processes would also do so in reality 11:58 h.

270

275

280



285 **Figure 2: Clusters found in diel residuals of nitrate (NO_3^-) concentration (C_{res}) and its derivative (δC_{res}). While the C_{diel} . Capital letters above panels are cluster names ordered alphabetically according to cluster size. Black lines indicate median diel patterns are, shaded areas indicate the 5th to 95th percentile. Note that C_{diel} reflects deviations from the 24 h floating average so that negative values do not clearly related to different imply that negative concentration levels of nitrate, they are characterized by were observed.**

290 Throughout the season, NO_3^- concentrations ranged between 2.47 mg L⁻¹ and 7.44 mg L⁻¹ (Fig. 3). Mean values and standard deviations at the three monitoring sites were 4.64 ± 0.66 mg L⁻¹ (S1), 4.63 ± 0.73 mg L⁻¹ (S2), and 4.36 ± 0.75 mg L⁻¹ (S3). Considering only days with complete upstream and downstream observations, i.e. comparing averages of the same day, NO_3^- concentration significantly increased between S1 and S2 (from 4.61 to 4.86 mg L⁻¹, $p < 0.001$, $n = 42$) and significantly decreased between S2 and S3 (from 4.54 to 4.40 mg L⁻¹, $p < 0.001$, $n = 121$) (Fig. S2). Daily averages of NO_3^- were negatively correlated with water level ($\rho = -0.34$, $p < 0.001$), positively with water temperature ($\rho = -0.53$, $p < 0.001$), and uncorrelated with global

295 irradiance ($\rho=0.01$, $p=0.93$). The overall negative correlation between NO_3^- and water level was dominated by large floods in May and June. Particularly in the second half of the study period, e.g., in early August (S2 and S3) and late October (S1 and S2), NO_3^- concentrations increased in response to floods (Fig. 3). Daily NO_3^- amplitudes were neither correlated with water level ($\rho=-0.03$, $p=0.76$), water temperature ($\rho=0.11$, $p=0.22$), nor with global irradiance ($\rho=-0.07$, $p=0.21$).

In terms of cluster occurrence, a largely similar seasonal pattern was apparent at all monitoring sites, despite different numbers
300 of recorded days. Cluster A dominated in May and again in October and was replaced by cluster B during the summer months from June to September. Both clusters usually formed continuous blocks of several days. Cluster C occurred occasionally throughout the season but preferentially in early summer, while cluster D and E mainly occurred in fall. On most days (62.0%), diel NO_3^- recordings at the upstream and downstream monitoring sites were attributed to the same cluster. However, longitudinal stability was different in the stream reaches (50.0% in the upper and 66.1% in the lower reach) and among clusters.
305 Cluster A was most stable (84.2%, $n=57$), while cluster B (62.3%, $n=53$) and C (61.9%, $n=21$) were close to the average. Cluster D (28.6%, $n=14$) and cluster E (12.5%, $n=16$) turned out to be comparatively unstable.

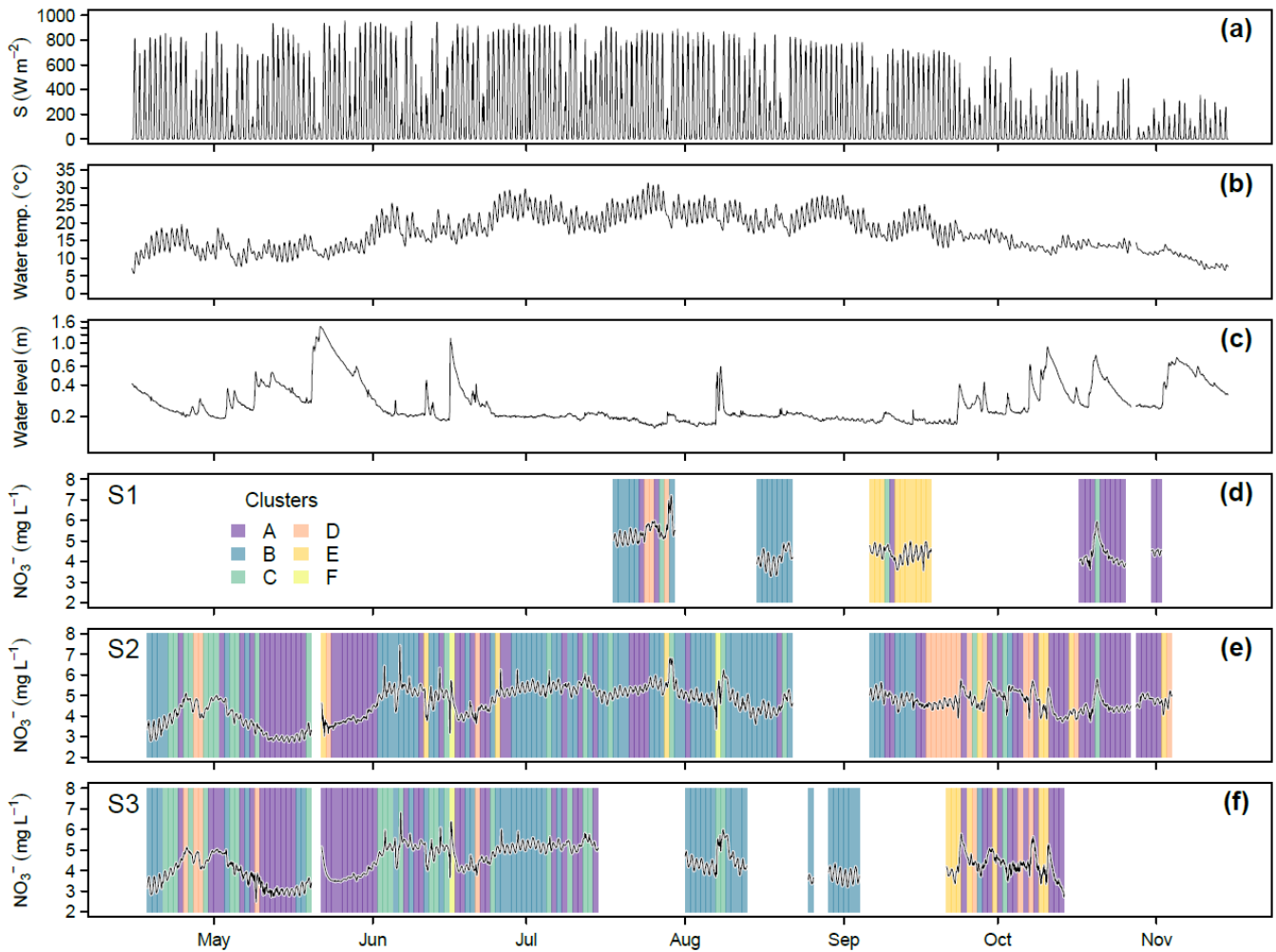


Figure 3: Global irradiance (a), water temperature (b) and water level (c) at S3 as well as NO_3^- concentration and cluster occurrence at the monitoring sites S1 (d), S2 (e), and S3 (f). Background colors in panels d to f indicate to which cluster the corresponding day was assigned.

310

3.2 In-stream vs. transport control on diel patterns

The time lags between diel NO_3^- signals at adjacent monitoring sites were usually shorter than the solute travel times between the stations. The salt dilution measurement resulted in a discharge of $2.0 \text{ m}^3 \text{ s}^{-2}$ resulted in travel time (τ_a) estimates of 2.0 h in the upper and 2.3 h in the lower reach (Fig. 4). Estimates of nominal residence time (τ_n) resulted in a range of plausible values and displayed increasing travel times with decreasing stream flows. The fact that the independently determined τ_a was included in the range of τ_n , showed that the estimated travel times were plausible. In both reaches the time lags between the concentration signals roughly ranged between zero and the travel time estimates, but were significantly different from both zero ($p < 0.001$,

315

both reaches) and minimum travel time ($p < 0.001$, both reaches). In the lower reach, lags formed an evenly distributed point cloud. Within this cloud, Cluster D, E, and F only appear at above median flows. In the upper reach, time lags were concentrated towards the extremes, i.e. either close to zero or close to travel time estimates. Days with below median stream flow were mainly assigned to cluster B and those above median stream flow to cluster A.

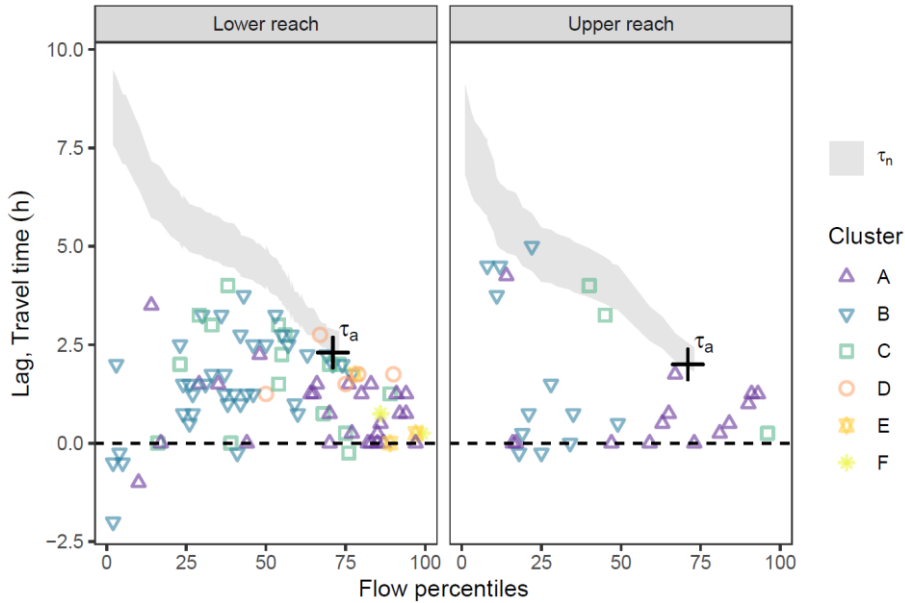
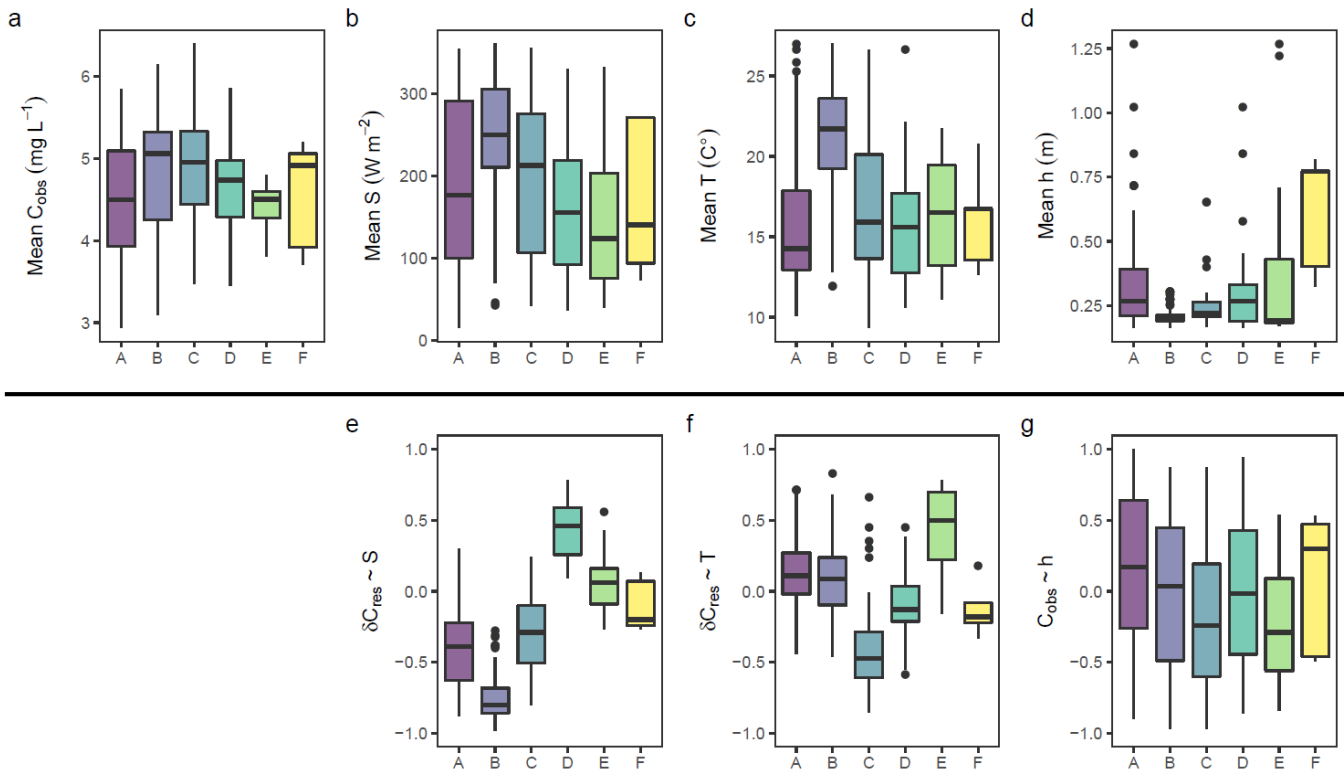


Figure 4: Travel time between diel NO_3^- signals at adjacent monitoring points compared to the tracer travel time (τ_a , black cross) and the range of nominal travel time estimates (τ_n , shaded area). No travel times were estimated when discharge exceeded the validity range of the rating curve. The figure only shows lags determined from signals with a corresponding cross-correlation coefficient above 0.75 (84.0% of the days).

3.3 Characterization of clusters

We found clear differences in the distribution of daily means of environmental parameters among clusters (Fig. 5). Despite minor variability in NO_3^- concentration among clusters, cluster assignments were closely linked to global irradiance, water temperature and water level. The most distinct cluster (cluster B) showed the highest maximum solar radiation irradiance (median: 259825.0 W/m^2) and the highest water temperature (median: 21.7 °C). The other clusters emerged during lower water temperatures (median: 15.2 °C) and variable solar irradiation. Daily average water levels were lowest and strongest most clearly confined in cluster B (median: 20.1 cm) and highest in cluster F (median: 77.2 cm), while the remaining clusters represented intermediate flow conditions. Further assessment of the diel dynamics of cluster A and C global irradiance sometimes reached similar high values as during cluster B but water temperature was lower. The clusters D and E reflected both lower irradiance and lower water temperature. Cluster F consisted of only 3 days, but all of these represented water levels hardly ever observed in the remaining clusters.

In addition to different environmental conditions, we identified different relationships with potential drivers revealed that δC_{res} of diel cycles among clusters (Fig. 6). The correlation of δC_{diel} and S was positively correlated with solar radiation positive in cluster D (Fig. 4e), and negatively, negative in clusters A, and C, and especially strongly in cluster B. negative in cluster B. Moderate correlations of δC_{diel} and T were found in cluster C (negative) and cluster E (positive). Correlations of δC_{res} with temperature appear in cluster C (negative) and cluster E (positive) (Fig. 4f). Correlations of nitrate concentrations with diel water level fluctuations (Fig. 4g), despite being high in some cases, are not δC_{diel} with h were weak and difference among clusters were less pronounced than with S and T. The relationship of C_{obs} and h was very systematic and show a high variability in all clusters. variable and included both strongly positive and negative correlations. However, strong overlapping of boxplots in Fig. 6c and Fig. 6d indicated that variability within clusters was higher than among cluster.



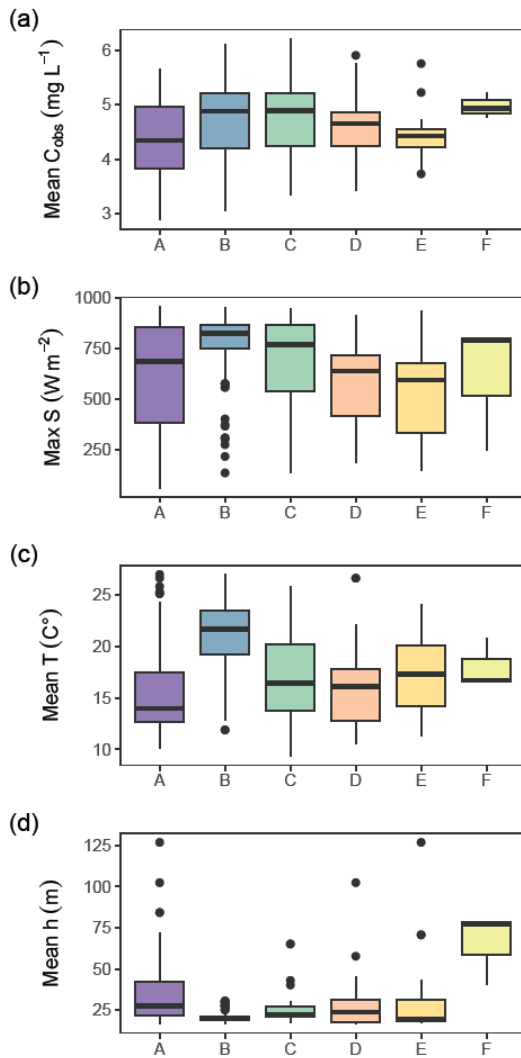
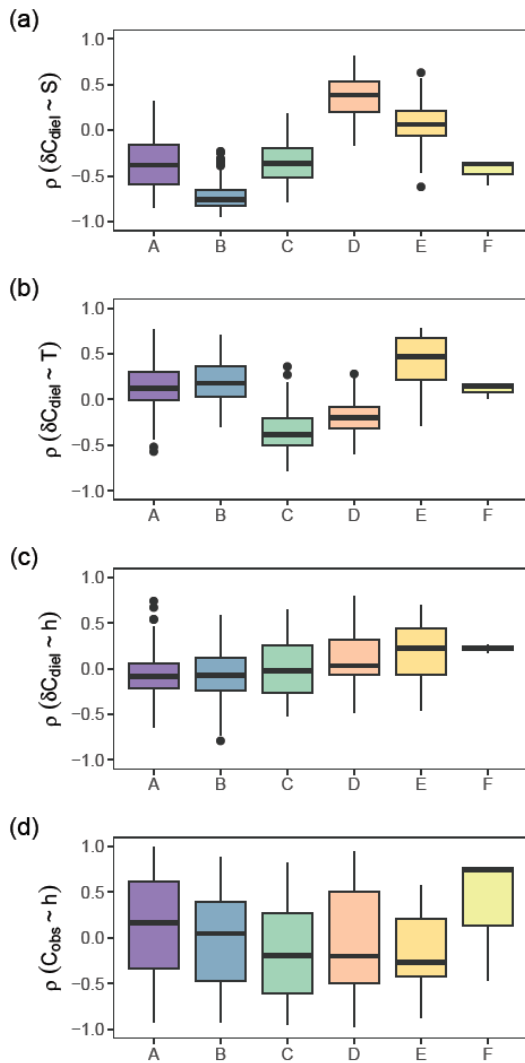


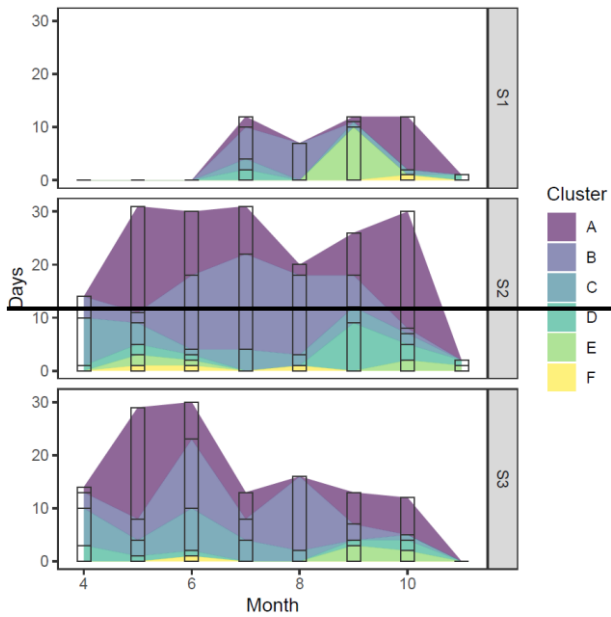
Figure 5: Properties of clusters and associated environmental conditions, during occurrence of clusters. The upper panels show daily means of measured nitrate concentration (a), daily maximum of global irradiance (b), daily average water temperature (c), and daily average water level- (d). The lower panels show daily Spearman rank correlation of the change rate of diel residual concentrations (δC_{res}) with irradiance (e) and water temperature (f) as well as daily correlations of measured concentration with water level (g).

The relationships of the clusters with the different environmental variables are reflected in their seasonal occurrence (Fig.



5) The general pattern is similar at all monitoring sites, but most clearly visible at the intermediate site S2 where the data set was most complete. From June to August the radiation-related cluster B dominates. In colder months in spring and fall the diel nitrate amplitude decreased and cluster A replaces cluster B. Cluster C appeared most often in early spring but continued to play a minor role throughout the entire season. Cluster D, E and F are marginally present throughout the season with a short continuous block of cluster D and E at sites S1 and S2, respectively, in September.

360



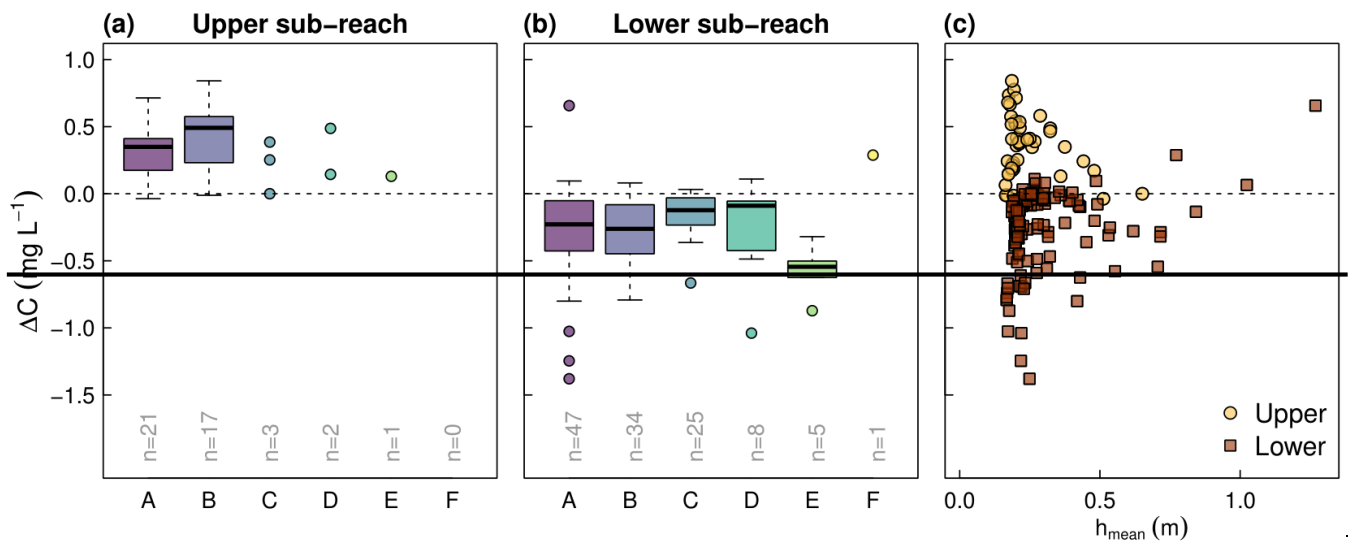
365

Figure 6: Seasonality of cluster occurrence

3.3 Relation of nitrate clusters reach balance

370

No relation was found between clusters and ΔC . In the upper sub reach (Fig. 6a), nitrate concentrations increased in almost all cases. Median nitrate surplus was 0.35 mg L^{-1} in cluster A and 0.49 mg L^{-1} in cluster B. In the lower sub reach a deficit was observed for most days (Fig. 6b). Decreases in median concentration ranged between -0.09 (cluster C) and -0.54 mg L^{-1} (cluster E). In both sub reaches, imbalance is most pronounced during low water levels (Figure 6c), i.e. low flow conditions, and decreased for higher water levels.



375 **Figure 6: Sub-reach balance of nitrate concentrations by cluster attributed to the corresponding downstream monitoring point and compared to water level (h_{mean}) as well as daily net change in nitrate by cluster.**

: Daily Spearman correlations of the NO_3^- signal with potential drivers by cluster. The panels show correlation strength of diel concentration change rate with global irradiance (a), diel concentration change rate with water temperature (b), diel concentration change rate with water level (c), and observed concentration with water level (d).

4 Discussion

380 4.1 Prevalence of in-stream processes in creation of diel General patterns

We found that travel times calculated from the diel nitrate signals at the monitoring points were usually between zero and the estimated water travel time (Fig 2). However, lags only exceeded our estimate of minimum travel time in a few cases. These data points were often associated with a low cross-correlation and hence less reliable for time lag estimation. On the one hand, spatial heterogeneity in environmental conditions and stream properties may cause some transformation of solute signals despite spatial synchrony in biochemical processes (e.g. start of photosynthesis may be delayed in temporary shaded areas), explaining lags scattering around zero. On the other hand, solutes cannot travel faster than water and travel time will increase with decreasing flow. Our estimates of minimum nominal water travel time can be considered conservative in the sense that plug flow (maximum flow velocity) was assumed and no factors were included that may further delay solute transport when water levels decrease, e.g. reduced short-circuiting. Downstream transport of solute signals therefore fails to explain most of our data. We therefore interpret our data to indicate primarily in-stream origin of diel nitrate cycles.

385
390

In-stream biotic control on nutrient biogeochemistry was also stated by Roberts and Mulholland (2007) in a forest stream in Tennessee, US. A simulation of longitudinal evolution of diel nitrate patterns by Hensley and Cohen (2016) showed that a distance of tens of kilometers can be required for nitrate concentration from a constant source to converge to a stable diel pattern. During convergence, they observed that the timing of the daily nitrate minimum oscillated with a longitudinal period of about 11 km, corresponding to the mean distance travelled in 24 h, i.e. distance between extremes was 5.5 km. This distance is comparable to the distance between monitoring sites in our study (5.7 km from S1 to S3) and flow length from the main source area of the river Elz to the monitored stretch (~45 km) was also comparable to the convergence distance observed by Hensley and Cohen (2016). It therefore seems plausible that longitudinal stability of diel nitrate patterns was not yet fully reached at our monitoring sites and the observed differences in timing (time lags > 0 in Fig. 2) were due to longitudinal variability in the diel nitrate signal. However, convergence distance in such a model may depend on transport parameters and residence time in the simulated stream reach. Hence, further research is needed to investigate the influence of river hydraulics on the diel solute patterns.

4.2 — Which processes may cause the observed diel nitrate patterns?

According to Nimick et al. (2011), diel nitrate concentrations reported in literature are usually characterized by a minimum in the early evening and a maximum just before dawn as represented by cluster A and B in our study, accounting for 69.6 % of all measured days (n=355). Such patterns are often attributed to nitrate uptake by primary producers. In our study the strong negative correlation between δC_{res} and global radiation, which was observed in cluster B (and to a minor extend also in cluster A), points in the same direction. The interpretation of the remaining clusters is more complex. While cluster E and F are strongly influenced by unstable discharge conditions and should not be interpreted in regard to instream processes due to non-stationary conditions, flow was stable in clusters C and D. These clusters were characterized by midday and evening concentration peaks, respectively. Possible explanations for the deviation of these clusters from the general pattern of morning peaks and afternoon minima are that either our assumptions on the diel course of plant uptake were violated (i.e. assimilatory uptake was not a function of insolation) or that variability in timing observed in these clusters was driven by microbial processes rather than plant uptake.

4.2.1 — Assimilatory uptake likely varies in intensity but not in timing

If plant uptake was the only control on diel nitrate patterns, variability in clusters would indicate temporal shifts in plant uptake that could either evolve from shifts in drivers of photosynthesis or from rate limitations caused by factors other than temperature or light availability. Drivers of photosynthesis did not undergo, despite a minor seasonal effect, systematic time shifts in this study. Neither did canopy development reduce light availability as observed in other studies (Rusjan and Mikoš, 2010; Roberts and Mulholland, 2007) due to absence of a forest or large trees near the stream, nor did certain clusters represent a typical weather condition such as e.g. days with cloudy morning and sunny afternoon. If that would be the case, correlations

of δC_{res} with drivers of photosynthesis should have been more or less equal for all clusters. We found that such correlations were clearly different among the clusters (Fig. 4), indicating that photosynthesis related plant uptake was not the only control on nitrate processes and thus the formation of diel nitrate patterns.

Plant uptake, however, may be temporarily limited by factors other than light availability, e.g. by limitation of other nutrients such as phosphorous. Phosphorus was not continuously measured, however, we did not observe phosphate concentrations $> 0.5 \text{ mg-L}^{-1}$ in longitudinal grab samples (as measured with IC). The interplay between diel nitrate and phosphorus cycles is not fully investigated. Cohen et al. (2013) found temporal decoupling of phosphorus and nitrate uptake in the Ichetucknee River (Florida, USA). Yet, phosphorus was not considered a limiting factor in their ecosystem. Mesocosm experiments by Chamberlin et al. (2019) on the effect of nutrient limitation on nitrate uptake showed that P limitation caused reduction of primary production but the influence on diel nitrate uptake remained unclear. We assume that if phosphorus became limiting at some point of time and its uptake less efficient, this would rather cause nitrate uptake to slowly fade out but not to stop abruptly. Then phosphorus limitation would influence the overall intensity of nitrate uptake rather than its diel pattern. We therefore conclude that timing of assimilatory nitrate uptake, in contrast to intensity, most likely did not undergo substantial changes throughout the season.

4.2.2 — Variability in microbial nitrate pathways likely cause variability in timing

An alternative explanation for the variability in diel cycles could be a dominance of microbial nitrate production or depletion. This would require diel variability in timing of microbial processing. In fact, diel variability was reported for both nitrification and denitrification. Denitrification rate was reported to be reduced during daytime when oxygen levels are high (Christensen et al., 1990; Harrison et al., 2005). Nitrification rates, in contrast, were found to increase with oxygen availability (Dunn et al., 2012; Laursen and Seitzinger, 2004) and depend on pH and temperature (Warwick, 1986). Nitrification can also enhance denitrification in freshwater (Lorenzen et al., 1998) or marine sediments (Marchant et al., 2016) so that denitrification resulting from coupled nitrification-denitrification at an aerobic-anaerobic boundary may, despite unfavorable water column oxygen levels, be stronger during day than during night. Recently, Hensley and Cohen (2020) observed evidence for diel variation in non-assimilatory pathways such as denitrification and nitrification in stream chamber experiments. Lupon et al. (2020) observed spatial variability in nitrification in boreal streams in response to inputs of labile organic carbon. As microbial nitrate processing may happen via these different pathways, the likelihood that changes in environmental conditions cause variability in the dominance among these processes and thereby variability in timing of net processing rate is considered greater than in the case of assimilatory plant uptake.

4.2.3 — Dominance of microbial nitrate processing

The above suggests that at least in the formation of clusters C and D, microbial processes dominate over primary production and therefore can imprint their diel course on the nitrate concentrations during these days. However, this is only true, if no plant uptake occurs at night, i.e. all plant uptake happens at daytime and contributes to the formation of corresponding diel patterns. Zero plant uptake at night is a common assumption in studies that aim to estimate nitrate processing rates from high frequency data by interpolating between night time maxima of nitrate concentration (Heffernan and Cohen, 2010). However, Mulholland et al. (2006) determined nitrate uptake in two streams by tracer ^{15}N NO_3^- addition and found that uptake at night was smaller than during the day but not zero. This finding was attributed to continued uptake by algae until photosynthate reserves accumulated during daytime photosynthesis were depleted. If such reserves are indeed depleted during the night, the assumption of zero plant uptake at night remains valid. If, however, baseline plant uptake occurs at night, the relative importance of plant uptake would be underestimated.

In contrast to plant uptake, rates of opposed microbial processes (e.g. of nitrification and denitrification) may partially cancel each other out. However, if microbial processing generally dominates over plant uptake, minor relative changes in microbial processing might strongly influence diel nitrate patterns and thus increase the likelihood to observe variability in such patterns. In fact, dominance of denitrification over plant uptake has been found in other studies. Heffernan et al. (2010) found that assimilatory uptake was responsible for about 20% of total nitrate removal in the Ichetucknee River (Florida, USA) and attributed the remainder mainly to denitrification. Recently, a similar ratio was found by Preiner et al. (2020) in three reaches with different macrophyte density in the river Fischa (Austria).

4.2.4 — Interpretation of individual clusters

The suggested dominance of microbial processes in in stream nitrate processing has implications for the interpretation of the diel nitrate patterns observed in this study. The diel course of microbial nitrate processing rates has to adopt a shape complementary to plant uptake so that the combination of both rates (δC_{res} in Fig. 3) can reproduce the observed concentration patterns. Diel patterns such as those observed in cluster A are often attributed to primary production and associated plant uptake. The fact that diel change rate in concentrations closely reflected patterns in insolation as observed in this study and also in stream chamber experiments by Hensley and Cohen (2020) invites to this interpretation. However, the effects of plant uptake and denitrification cannot be separated, if both processes work synchronously. Increasing amplitudes from cluster A to B suggest a superposition of both nitrate depleting processes particularly during times of reduced flow velocity at low water levels associated with cluster B. Then a larger fraction of water interacts with stream sediments where denitrification occurs. Although similar diel patterns are often simply attributed to assimilatory uptake, Heffernan et al. (2010) argued that denitrification may be promoted by algal exudates which are rich in labile organic matter and are released during

photosynthesis (Wyatt et al., 2012). If such exudates are released by benthic algae, labile organic matter might relatively quickly diffuse into anoxic zones of river sediments and promote denitrification.

485

Depending on how quickly such zones in the sediment (hyporheic zone) are reached, the resulting peak in denitrification will lag behind the peak of primary production and produce a nitrate concentration pattern like that observed in cluster C. Shifts in diel nitrate patterns similar to those between cluster A and B on the one hand and cluster C on the other hand were observed at a seasonal scale by Rusjan and Mikoš (2010). They attributed this finding to inhibition of photosynthesis and associated plant uptake by low morning water temperatures in spring and fall. This, however, was not the case in our study, since water temperatures did not regularly fall below the threshold of 10 °C referred to by Rusjan and Mikoš (2010). Furthermore, the temperature range of cluster C did not differ much from the remaining clusters (Fig. 4), except for cluster B. The exact circumstances that caused the formation of cluster C in our study therefore remain unclear.

490

495

The opposite behavior than in cluster A and B was observed in cluster D where a perfect synchrony of nitrification and plant uptake may have caused partial extinction so that a net nitrate production was observed. Similar patterns were found by Hensley and Cohen (2020) during nitrate limitation. Although in our study the reason for low plant uptake is certainly not nitrate limitation, this shows that microbial nitrate processing, i.e. nitrification in this case, may become dominant and imprint its diel variability on nitrate concentrations, if plant uptake is low. Nitrate maxima during the second half of the day were also found by Aubert and Breuer (2016) during summer in two different years.

500

4.2.5 — Implications for seasonality of nitrate processing

The above interpretation of the clusters has implications for the seasonal dominance of certain nitrate processing pathways (Fig. 5). Moderate daytime dominance of nitrate depleting processes occurred mainly in spring and fall (cluster A). Daytime dominance of nitrate depleting processes increased in the summer months (cluster B) when both solar radiation and temperature were highest. During this period synchrony in plant uptake and (possibly coupled by photosynthetic exudates) denitrification may have caused the highest daily concentration amplitudes, except for the disturbed clusters E and F. Cluster C occurred less frequently than cluster A and B but throughout the season and preferentially in spring and early summer. Patterns suggesting daytime dominance of nitrate production, i.e. nitrification, occurred several days in early and late summer (cluster D). A seasonal pattern in nitrate cycles was also found by Roberts and Mulholland (2007) who attributed highest amplitudes to gross primary production, i.e. plant uptake. However, due to dense forest coverage of the investigated stream, maximum amplitudes occurred earlier in the year than at our exposed study site. Aubert and Breuer (2016) associated seasonal shifts in diel nitrate cycles with diel fluctuations in discharge induced by evapotranspiration. We consider this explanation highly unlikely in the investigated system as no consistent diel cycles in discharge were observed.

505

510

4.3 — Reach balance dominated by external processes

515 No relationship was found among clusters and ΔC but ΔC was clearly different in both sub reaches across all clusters. This suggests that nitrate mass balances of the sub reaches were overridden by processes that affected nitrate concentrations regardless of cluster occurrence. These processes might be lateral inflows or groundwater exfiltration, not considered so far in our interpretation. In the upper sub reach we identified a tributary as a potential nitrate source in which snapshot sampling on a hot day during low flow conditions revealed nitrate concentration to be twice as high as in the main stream. The negative nitrate balance between S2 and S3 may be the result of biological net nitrate removal. Moreover, the increase between S1 and S2 and subsequent decrease towards S3 reflects the regional pattern of nitrate concentration in the groundwater monitoring wells measured by the state agencies. Regional groundwater wells upstream of S2 typically show higher concentrations than in stream water, while nitrate concentrations in wells downstream of S2 are mainly lower than stream water concentrations. Groundwater influence was originally considered minimal in the study reach due to the presence of drainage ditches along the outside of the levees on both sides of the stream, collecting lateral groundwater flowing to the stream. However, longitudinal sampling with high spatial resolution and infrared imagery suggested the presence of groundwater inflow zones in the lower sub reach. The explanation of nitrate reach imbalances by unconsidered inflows is in line with the observation that in both reaches nitrate imbalance was greatest during phases of low flow when inflows of limited volume but strongly deviating concentrations cause maximum effects (Fig. 6c).

530 In our data we found patterns in NO_3^- concentration both on the diel and on the seasonal scale. On the seasonal scale, a weak negative correlation of NO_3^- and water level indicated that flow events tend to dilute NO_3^- concentrations in our river. However, particularly after the low flow period in summer, NO_3^- increased during discharge events, an observation that is often explained by the mobilization of previously accumulated NO_3^- in soils (Burns et al., 2019; Lange and Haensler, 2012). The fact that NO_3^- was correlated with stream temperature but not with global irradiance may be a consequence of a more intense seasonal pattern in water temperature than in irradiance, since we started our monitoring campaign in late spring when daily irradiance peaks were already close to their seasonal maximum. On the diel scale we identified six different NO_3^- patterns that varied seasonally. Interestingly, daily amplitudes of these patterns did not show correlations with daily averages of light intensity, water temperature or water level. The fact that longitudinal stability varied among cluster suggests that less stable clusters (e.g. D and E) either indicated a shift in in-stream conditions or external controls on diel patterns, e.g. transport.

540 4.2 In-stream vs. transport control

The comparison of time lags between monitoring sites with travel time revealed that lags were usually too small to be produced by transport alone, but higher than expected for the case of pure in-stream control (Fig. 4). The existence of lags may thus be caused by an interaction of transport and in-stream processes. Simulating the longitudinal evolution of NO_3^- concentration downstream of a constant source, Hensley and Cohen (2016) found that timing of NO_3^- extremes was variable in the proximity

545 of the source, but with increasing travel distance, NO_3^- concentration converged into a stable signal solely defined by in-stream
processing. Depending on the position of observation points along such a stream reach, one may find time lags like those
observed at our river Elz. Although boundary conditions at our study site are far less constrained than in the simulation of
Hensley and Cohen (2016), their results might principally explain our observed time lags. Non-zero lags would then indicate
that at the study site NO_3^- concentration had not yet fully converged and was still partially influenced by transport.
550 Nevertheless, observed time lags were clearly smaller than estimated travel times. We therefore conclude that the observed
diel NO_3^- patterns were not primarily produced by transport processes.

4.3 Lateral inputs

Diel NO_3^- patterns may also be influenced by lateral inputs, including tributaries and groundwater interaction. The only surface
tributary within the studied stream reach was between S1 and S2. It was initially considered negligible and therefore not
555 accounted for. However, snap shot sampling on a hot day during low flow conditions revealed nitrate concentration to be twice
as high as in the main stream. It is also possible that groundwater influx influenced NO_3^- concentration at the monitoring sites.
In fact, NO_3^- levels in groundwater were higher than in stream water in the proximity of the upper reach and lower than in
stream water along the lower reach (Fig. S3). Although the overall flow direction of groundwater was parallel to the stream,
groundwater inputs might explain the increase in average NO_3^- concentration from S1 to S2 and subsequent decrease from S2
560 to S3 (Fig. S2). Previous research identified diffuse groundwater inputs as a considerable challenge for determining mass
balances using paired high-frequency probes (Kunz et al., 2017). We were unable to separate the effects of groundwater inputs
from a potential effect of increased NO_3^- removal in the lower reach due the revitalization measures.

Although lateral inputs may have affected average NO_3^- levels, their influence on diel NO_3^- patterns was only marginal. In the
upper reach, which received the tributary, diel NO_3^- patterns were mostly longitudinally stable, except for the deployment in
565 September (Fig. 3). We therefore consider the influence of the tributary to be limited. Riparian groundwater interaction induced
by evapotranspiration was suggested by Aubert and Breuer (2016) to explain a seasonal shift in diel NO_3^- patterns. Flewelling
et al. (2014) showed that diel fluctuations in groundwater level and stream flow induced by evapotranspiration may be
sufficient to produce measurable diel patterns in stream NO_3^- concentration. Groundwater inputs may not only directly affect
 NO_3^- concentrations but also alter stream chemistry, e.g., by introducing labile organic carbon which promotes heterotrophic
570 processes (Lupon et al., 2020). In the present study, however, diel water level fluctuations were usually minimal so that we
generally have little evidence for diel variability in groundwater influx.

4.4 Interpretation of diel patterns

Diel NO_3^- patterns with a maximum in the early morning and a minimum in the afternoon are usually explained by
photoautotrophic NO_3^- uptake by primary producers (Nimick et al., 2011). This was also the largest group of diel patterns in
575 our study including cluster A and B, jointly accounting for about 70 % of the data. In our study, the idea that such diel patterns

reflect photoautotrophic uptake is supported by a strongly (cluster B) and moderately (cluster A) negative correlation between δC_{diel} and global irradiance. The higher amplitude of cluster B (Fig.2) suggests a stronger photoautotrophic NO_3^- uptake compared to cluster A. Consequently, the seasonality in cluster occurrence suggests that photoautotrophic NO_3^- uptake was strongest from June to early September when cluster B prevailed. In May and October the dominance of cluster A suggests reduced photoautotrophic NO_3^- uptake which may be due to reduced light availability in autumn or due to lower water temperatures and higher flow during both periods. The latter may have influenced photoautotrophic NO_3^- uptake via reduced light penetration through a higher water layer, via an increased volume of water on which the same uptake in terms of mass would have a smaller impact in terms of concentration, and via disruption of stream metabolism due to destruction of vegetation by flood events (Burns et al., 2019).

Patterns with a midday maximum such as those observed in cluster C have also been explained by photoautotrophic uptake in streams where timing of light availability changed seasonally with canopy development (Rusjan and Mikoš, 2010; Roberts and Mulholland, 2007; Rode et al., 2016). Although global radiation was comparatively intense during occurrence of cluster C and δC_{diel} was weakly correlated with global irradiance, this explanation seems unlikely in our river reaches, since banks are unforested and the seasonal occurrence of cluster C did not correspond to canopy development. Despite being most obvious, diel variability is not exclusively caused by photoautotrophic uptake and has been observed in other biochemical processes of the nitrogen cycle (Hensley and Cohen, 2020), such as nitrification (Warwick, 1986; Laursen and Seitzinger, 2004; Dunn et al., 2012) and denitrification (Christensen et al., 1990; Harrison et al., 2005; Cohen et al., 2012). The interplay of these processes can be regulated by oxygen availability (Rysgaard et al., 1994), i.e. nitrification and denitrification are expected to be most intense during oxygen maxima and minima, respectively. In addition, microbial processes may vary with water temperature fluctuations that propagate into the hyporheic zone and influence the rate of microbial processes (Zheng and Bayani Cardenas, 2018). Timing of nitrification and denitrification may also be shifted relative to photosynthesis and photoautotrophic uptake due to oxygen-dependency of nitrification and denitrification and due to travel time to reactive zones in stream sediments.

Considering that denitrification was found to be the dominant pathway of NO_3^- removal in some streams (Preiner et al., 2020; Heffernan et al., 2010), it seems possible that varying diel NO_3^- patterns are caused by variability in denitrification or nitrification rather than in photoautotrophic uptake. Following this line of thought, negative (cluster C) and positive (cluster E) correlations of δC_{diel} with stream water temperature suggest that nitrification and denitrification, respectively, may be the underlying processes. In that case higher light inputs during cluster C compared to cluster E (Fig. 5) may have caused higher photosynthetic oxygen availability and thus a dominance of aerobic nitrification over anaerobic denitrification. Diel patterns with peaks in the afternoon or evening such as those in cluster D have been observed by Hensley and Cohen (2020) during NO_3^- limitation, which was obviously not the case in the present study. Similar patterns to cluster D were also found by Aubert and Breuer (2016) and Flewelling et al. (2014) in streams subject to intense evapotranspiration which has been shown to influence hydrologic retention of NO_3^- (Lupon et al., 2016). Although diel water level fluctuations were usually minimal, this may have been the case during the persistent occurrence of cluster D at S2 after a prolonged dry period in September (Fig. 3).

610 These findings suggest that, despite a dominance of photoautotrophic assimilation, other processes contribute to the formation
of diel NO_3^- patterns in the river Elz. These may be contrary processes like nitrification and denitrification and possibly also
physical processes like diel variability in lateral inputs induced by evapotranspiration. The relative importance of these
processes varies seasonally and is reflected in shifts of diel NO_3^- patterns. Although the distinct clusters identified in our
analysis invite for speculation, in-stream NO_3^- processing is complex and processes may overlap and interact which makes
615 unambiguous interpretation solely based on NO_3^- recordings challenging.

4.4.5 Conclusions

Our study shows that diel nitrate patterns recorded at three locations in a 5.1 km long stream reach largely resulted from in-
reach processes. Downstream advection of upstream concentration perturbations was ruled out as an explanation for diel
patterns since time lags between monitoring sites determined by cross correlation were predominantly smaller than water travel
620 time estimates. Analysis of diel patterns revealed that approximately 70% of all diel patterns were attributed to two clusters
that were negatively related to the diel course of insolation with highest nitrate amplitudes on warm and sunny days and low
water levels. We suggest that these patterns were caused by synchronous denitrification and autotrophic nitrate uptake, relative
importance of which is unclear and may vary according to environmental conditions. In the remaining clusters temporal shifts
were evident that could be explained by temporal shifts in microbial nitrate processing but not by photosynthesis driven uptake.
625 In these cases, microbial processing rates need to be higher than assimilation rates in order to reproduce the observed patterns.
In summary, our study suggests that varying dominance and synchronicity of autotrophic assimilation and microbial processes
may cause different diel nitrate patterns in stream systems. In a 5.1 km stream reach of the river Elz in Southwest Germany we
identified diel patterns in stream NO_3^- concentration, differentiated between in-stream and transport control, and analyzed how
patterns were related to environmental conditions and potential drivers. We found a set of six clusters representing different
630 characteristic diel NO_3^- patterns. Relatively small temporal shifts between adjacent monitoring sites indicated that NO_3^-
concentration patterns were predominantly formed by in-stream processes and not by a transport of upstream NO_3^- inputs.
Most patterns were characterized by a pre-dawn maximum and an afternoon minimum of varying intensity, and mostly the
change rate of NO_3^- concentration was negatively correlated with global irradiance. We therefore conclude that these patterns
were primarily produced by photoautotrophic NO_3^- uptake. However, we also found indications that other biochemical
635 processes like nitrification and denitrification contributed to the formation of NO_3^- patterns. In depth interpretation and
eventually quantification of process rates would require spatially distributed high frequency information on stream metabolism,
e.g. dissolved oxygen concentrations, and on different N species, most importantly NH_4^+ . Nevertheless, our analysis suggests
that particular combinations of different in-stream processes may generate distinct diel NO_3^- patterns. A seasonal shift in
patterns may then indicate shifts in the relative importance of the underlying processes. The clustering method used in this
640 study proved useful for making the data set accessible for this kind of analysis and may be used as a blueprint for the analysis
of other stream solutes.

|

References

- 645 Aubert, A. H. and Breuer, L.: New Seasonal Shift in In-Stream Diurnal Nitrate Cycles Identified by Mining High-Frequency Data, *PLoS One*, 11, e0153138, doi:10.1371/journal.pone.0153138, 2016.
- Austin, B. J. and Strauss, E. A.: Nitrification and denitrification response to varying periods of desiccation and inundation in a western Kansas stream, *Hydrobiologia*, 658, 183–195, doi:10.1007/s10750-010-0462-x, 2011.
- Birgand, F., Skaggs, R. W., Chescheir, G. M., and Gilliam, J. W.: Nitrogen Removal in Streams of Agricultural
- 650 Catchments—A Literature Review, *Crit. Rev. Env. Sci. Tec.*, 37, 381–487, doi:10.1080/10643380600966426, 2007.
- Burns, D. A., Pellerin, B. A., Miller, M. P., Capel, P. D., Tesoriero, A. J., and Duncan, J. M.: Monitoring the riverine pulse: Applying high-frequency nitrate data to advance integrative understanding of biogeochemical and hydrological processes, *WIREs Water*, 140, e1348, doi:10.1002/wat2.1348, 2019.
- ~~Chamberlin, C. A., Bernhardt, E. S., Rosi, E. J., and Heffernan, J. B.: Stoichiometry and daily rhythms: experimental~~
- 655 ~~evidence shows nutrient limitation decouples N uptake from photosynthesis, *Ecology*, 100, e02822, doi:10.1002/ecy.2822, 2019.~~
- Christensen, P. B., Nielsen, L. P., Sørensen, J., and Revsbech, N. P.: Denitrification in nitrate-rich streams: Diurnal and seasonal variation related to benthic oxygen metabolism, *Limnol. Oceanogr.*, 35, 640–651, doi:10.4319/lo.1990.35.3.0640, 1990.
- 660 Cohen, M. J., Heffernan, J. B., Albertin, A., and Martin, J. B.: Inference of riverine nitrogen processing from longitudinal and diel variation in dual nitrate isotopes, *J. Geophys. Res. Biogeo.*, 117, 758, doi:10.1029/2011JG001715, 2012.
- ~~Cohen, M. J., Kurz, M. J., Heffernan, J. B., Martin, J. B., Douglass, R. L., Foster, C. R., and Thomas, R. G.: Diel phosphorus variation and the stoichiometry of ecosystem metabolism in a large spring fed river, *Ecol. Monogr.*, 83, 155–176, doi:10.1890/12-1497.1, 2013.~~
- 665 ~~Covino, T. P., McGlynn, B. L., and McNamara, R. A.: Tracer Additions for Spiraling Curve Characterization (TASCC): Quantifying stream nutrient uptake kinetics from ambient to saturation, *Limnol. Oceanogr. Methods*, 8, 484–498, doi:10.4319/lom.2010.8.484, 2010.~~
- Derrick, T. R. and Thomas, J. M.: *Time-Series Analysis: The cross-correlation function*, Kinesiology Publications, 189–205, 2004.
- 670 Dodds, W. and Smith, V.: Nitrogen, phosphorus, and eutrophication in streams, *IW*, 6, 155–164, doi:10.5268/IW-6.2.909, 2016.
- Duan, S., Powell, R. T., and Bianchi, T. S.: High frequency measurement of nitrate concentration in the Lower Mississippi River, USA, *J. Hydrol.*, 519, 376–386, doi:10.1016/j.jhydrol.2014.07.030, 2014.
- Dunn, R. J.K., Welsh, D. T., Jordan, M. A., Waltham, N. J., Lemckert, C. J., and Teasdale, P. R.: Benthic metabolism and
- 675 nitrogen dynamics in a sub-tropical coastal lagoon: Microphytobenthos stimulate nitrification and nitrate reduction

- through photosynthetic oxygen evolution, *Estuarine Coastal Estuar. Coast. Shelf Sci.*, 113, 272–282, doi:10.1016/j.ecss.2012.08.016, 2012.
- Ensign, S. H. and Doyle, M. W.: Nutrient spiraling in streams and river networks, *J. Geophys. Res. Biogeo.*, 111, doi:10.1029/2005JG000114, 2006.
- 680 Gammons, C. H., Babcock, J. N., Parker, S. R., and Poulson, S. R.: Diel cycling and stable isotopes of dissolved oxygen, dissolved inorganic carbon, and nitrogenous species in a stream receiving treated municipal sewage, *Chem. Geol.*, doi:10.1016/j.chemgeo.2010.07.006, 2010.
- Flewelling, S. A., Hornberger, G. M., Herman, J. S., Mills, A. L., and Robertson, W. M.: Diel patterns in coastal-stream nitrate concentrations linked to evapotranspiration in the riparian zone of a low-relief, agricultural catchment, *Hydrol. Process.*, 28, 2150–2158, doi:10.1002/hyp.9763, 2014.
- 685 Grace, M. R., Giling, D. P., Hladyz, S., Caron, V., Thompson, R. M., and Mac Nally, R.: Fast processing of diel oxygen curves: Estimating stream metabolism with BASE (BAYesian Single-station Estimation), *Limnol. Oceanogr. Methods*, 13, e10011, doi:10.1002/lom3.10011, 2015.
- Grant, B. R.: The action of light on nitrate and nitrite assimilation by the marine chlorophyte, *Dunaliella tertiolecta* (Butcher), *J. Gen. Microbiol.*, 48, 379–389, doi:10.1099/00221287-48-3-379, 1967.
- 690 Harrison, J. A., Matson, P. A., and Fendorf, S. E.: Effects of a diel oxygen cycle on nitrogen transformations and greenhouse gas emissions in a eutrophied subtropical stream, *Aquat. Sci.*, 67, 308–315, doi:10.1007/s00027-005-0776-3, 2005.
- Hartigan, J. A. and Wong, M. A.: Algorithm AS 136: A K-Means Clustering Algorithm, *Applied Statistics App. Stat. J. Roy. St. C*, 28, 100, doi:10.2307/2346830, 1979.
- 695 Heffernan, J. B. and Cohen, M. J.: Direct and indirect coupling of primary production and diel nitrate dynamics in a subtropical spring-fed river, *Limnol. Oceanogr.*, 55, 677–688, doi:10.4319/lo.2010.55.2.0677, 2010.
- Heffernan, J. B., Cohen, M. J., Frazer, T. K., Thomas, R. G., Rayfield, T. J., Gulley, J., Martin, J. B., Delfino, J. J., and Graham, W. D.: Hydrologic and biotic influences on nitrate removal in a subtropical spring-fed river, *Limnol. Oceanogr.*, 55, 249–263, doi:10.4319/lo.2010.55.1.0249, 2010.
- 700 Hellwig, J., Stahl, K., and Lange, J.: Patterns in the linkage of water quantity and quality during low-flows, *Hydrol. Process.*, 31, 4195–4205, doi:10.1002/hyp.11354, 2017.
- Hensley, R. T. and Cohen, M. J.: On the emergence of diel solute signals in flowing waters, *Water Resour. Res.*, 52, 759–772, doi:10.1002/2015WR017895, 2016.
- Hensley, R. T. and Cohen, M. J.: Nitrate depletion dynamics and primary production in riverine benthic chambers, *Freshw. Sci.*, 39, 169–182, doi:10.1086/707650, 2020.
- 705 Kadlec, R. H.: Detention and mixing in free water wetlands, *Ecological Engineering*, 3(4), 345–380, doi:10.1016/0925-8574(94)00007-7, 1994.

- Kunz, J. V., Hensley, R., Brase, L., Borchardt, D., and Rode, M.: High frequency measurements of reach scale nitrogen uptake in a fourth order river with contrasting hydromorphology and variable water chemistry (Weiße Elster, Germany), *Water Resour. Res.*, 53, 328–343, doi:10.1002/2016WR019355, 2017.
- Lange, J. and Haensler, A.: Runoff generation following a prolonged dry period, *J. Hydrol.*, 464-465, 157–164, doi:10.1016/j.jhydrol.2012.07.010, 2012.
- Laursen, A. E. and Seitzinger, S. P.: Diurnal patterns of denitrification, oxygen consumption and nitrous oxide production in rivers measured at the whole-reach scale, *Freshwater Biol.*, 49, 1448–1458, doi:10.1111/j.1365-2427.2004.01280.x, 2004.
- ~~Lorenzen, J., Larsen, L. H., Kjær, T., and Revsbech, N. P.: Biosensor Determination of the Microscale Distribution of Nitrate, Nitrate Assimilation, Nitrification, and Denitrification in a Diatom Inhabited Freshwater Sediment, *Applied and Environmental Microbiology*, 64, 3264–3269, 1998.~~
- Lupon, A., Bernal, S., Poblador, S., Martí, E., and Sabater, F.: The influence of riparian evapotranspiration on stream hydrology and nitrogen retention in a subhumid Mediterranean catchment, *Hydrol. Earth Syst. Sci.*, 20, 3831–3842, doi:10.5194/hess-20-3831-2016, 2016.
- Lupon, A., Denfeld, B. A., Laudon, H., Leach, J., and Sponseller, R. A.: Discrete groundwater inflows influence patterns of nitrogen uptake in a boreal headwater stream, *Freshw. Sci.*, 0, doi:10.1086/708521, 2020.
- ~~Marchant, H. K., Holtappels, M., Lavik, G., Ahmerkamp, S., Winter, C., and Kuypers, M. M. M.: Coupled nitrification-denitrification leads to extensive N loss in subtidal permeable sediments, *Limnol Oceanogr*, 61, 1033–1048, doi:10.1002/lno.10271, 2016.~~
- Mulholland, P. J., Hall, R. O., Sobota, D. J., Dodds, W. K., Findlay, S. E. G., Grimm, N. B., Hamilton, S. K., McDowell, W. H., O'Brien, J. M., Tank, J. L., Ashkenas, L. R., Cooper, L. W., Dahm, C. N., Gregory, S. V., Johnson, S. L., Meyer, J. L., Peterson, B. J., Poole, G. C., Valett, H. M., Webster, J. R., Arango, C. P., Beaulieu, J. J., Bernot, M. J., Burgin, A. J., Crenshaw, C. L., Helton, A. M., Johnson, L. T., Niederlehner, B. R., Potter, J. D., Sheibley, R. W., and Thomasn, S. M.: Nitrate removal in stream ecosystems measured by ¹⁵N addition experiments: Denitrification, *Limnology and Oceanography*, 54(3), 666–680, doi:10.4319/LO.2009.54.3.0666, 2009.
- Mosley, L. M.: Drought impacts on the water quality of freshwater systems; review and integration, *Earth-Sci. Rev.*, 140, 203–214, doi:10.1016/j.earscirev.2014.11.010, 2015.
- Mulholland, P. J., Thomas, S. A., Valett, H. M., Webster, J. R., and Beaulieu, J.: Effects of light on NO₃⁻ uptake in small forested streams: diurnal and day-to-day variations, ~~*Journal of the North American Benthological Society*~~, *J. N. Am. Benthol. Soc.*, 25, 583–595, doi:10.1899/0887-3593(2006)25[583:EOLONU]2.0.CO;2, 2006.
- Nimick, D. A., Gammons, C. H., and Parker, S. R.: Diel biogeochemical processes and their effect on the aqueous chemistry of streams: A review, *Chem. Geol.*, 283, 3–17, doi:10.1016/j.chemgeo.2010.08.017, 2011.
- Pellerin, B. A., Downing, B. D., Kendall, C., Dahlgren, R. A., Kraus, T. E. C., Sacramento, J. F., Spencer, R. G. M., and Bergamaschi, B. A.: Assessing the sources and magnitude of diurnal nitrate variability in the San Joaquin River

(California) with an in situ optical nitrate sensor and dual nitrate isotopes, *Freshwater Biol.*, 54, 376–387, doi:10.1111/j.1365-2427.2008.02111.x, 2009.

745 Peterson, B. J., Wollheim, W. M., Mulholland, P. J., Webster, J. R., Meyer, J. L., Tank, J. L., Marti, E., Bowden, W. B., Valett, H. M., Hershey, A. E., McDowell, W. H., DODDS, W. K., Hamilton, S. K., Gregory, S., and Morrall, D. D.: Control of nitrogen export from watersheds by headwater streams, *Science (New York, N.Y.)*, 292, 86–90, doi:10.1126/science.1056874, 2001.

Pfenning, K. S. and McMahon, P. B.: Effect of nitrate, organic carbon, and temperature on potential denitrification rates in nitrate-rich riverbed sediments, *J. Hydrol.*, 187, 283–295, doi:10.1016/S0022-1694(96)03052-1, 1997.

750 Preiner, S., Dai, Y., Pucher, M., Reitsema, R. E., Schoelynck, J., Meire, P., and Hein, T.: Effects of macrophytes on ecosystem metabolism and net nutrient uptake in a groundwater fed lowland river, ~~The Science of the total environment~~, *Sci. Total. Environ.*, 721, 137620, doi:10.1016/j.scitotenv.2020.137620, 2020.

R Core Team: R: A language and environment for statistical, R Foundation for Statistical Computing, Vienna, 2019.

755 Roberts, B. J. and Mulholland, P. J.: In-stream biotic control on nutrient biogeochemistry in a forested stream, West Fork of Walker Branch, *J. Geophys. Res. Biogeo.*, 112, n/a-n/a, doi:10.1029/2007JG000422, 2007.

Rode, M., Halbedel Née Angelstein, S., Anis, M. R., Borchardt, D., and Weitere, M.: Continuous In-Stream Assimilatory Nitrate Uptake from High-Frequency Sensor Measurements, ~~Environmental science & technology~~, *Environ. Sci. Technol.*, 50, 5685–5694, doi:10.1021/acs.est.6b00943, 2016.

760 Rusjan, S. and Mikoš, M.: Seasonal variability of diurnal in-stream nitrate concentration oscillations under hydrologically stable conditions, *Biogeochemistry*, 97, 123–140, doi:10.1007/s10533-009-9361-5, 2010.

Rysgaard, S., Risgaard-Petersen, N., Niels Peter, S., Kim, J., and Lars Peter, N.: Oxygen regulation of nitrification and denitrification in sediments, *Limnol. Oceanogr.*, 39, 1643–1652, doi:10.4319/lo.1994.39.7.1643, 1994.

765 Scholefield, D., Le Goff, T., Braven, J., Ebdon, L., Long, T., and Butler, M.: Concerted diurnal patterns in riverine nutrient concentrations and physical conditions, ~~The Science of the total environment~~, *Sci. Total. Environ.*, 344, 201–210, doi:10.1016/j.scitotenv.2005.02.014, 2005.

Schwab, M.: Long-term, high-frequency analyses of the interplay between rainfall-runoff processes, discharge, DOC and nitrate, Doctoral dissertation, Albert-Ludwig-Universität, Freiburg, Germany, 2017.

Tan, P.-N., Steinbach, M., Karpatne, A., and Kumar, V.: Introduction to data mining, Second edition, Pearson, NY NY, 839 pp., 2019.

770 Trauth, N. and Fleckenstein, J. H.: Single discharge events increase reactive efficiency of the hyporheic zone, *Water Resour. Res.*, 53, 779–798, doi:10.1002/2016WR019488, 2017.

Warwick, J. J.: Diel variation of in-stream nitrification, *Water Res.*, 20, 1325–1332, doi:10.1016/0043-1354(86)90165-X, 1986.

775 Wyatt, K. H., Turetsky, M. R., Rober, A. R., Giroldo, D., Kane, E. S., and Stevenson, R. J.: Contributions of algae to GPP and DOC production in an Alaskan fen: effects of historical water table manipulations on ecosystem responses to a

~~natural flood, *Oecologia*, 169, 821–832, doi:10.1007/s00442-011-2233-4, 2012.~~ Zheng, L. and Bayani Cardenas, M.:
Diel Stream Temperature Effects on Nitrogen Cycling in Hyporheic Zones, *J. Geophys. Res. Biogeo.*, 123, 2743–2760,
doi:10.1029/2018JG004412, 2018.